RESILIENT INFRASTRUCTURE
June 1–4, 2016

WIND TESTING OF SPAN-WIRE TRAFFIC SIGNAL SYSTEMS

Peter Irwin
Florida International University, USA

Ioannis Zisis
Florida International University, USA

Benito Berlanga
Florida International University, USA

Bodhisatta Hajra
Florida International University, USA

Arindam Chowdhury
Florida International University, USA

ABSTRACT

Traffic signals are a critical part of the transportation infrastructure and it is important that they be robust enough to resist extreme wind storms lasting several hours. Failure of the signal systems results in unsafe traffic conditions during and after a storm, and the time taken for repairs delays recovery. A significant fraction of existing signals use span-wire supporting systems. The wire spans can range from 15 m to 60 m, depending on the width of the highway intersection, and exhibit nonlinear characteristics. The typical signal system used in Florida consists of the signal units, a catenary wire, hangers, a tensioned messenger wire, and the end support posts. The hangers are connected to the catenary wire at their upper ends and to the signal units at their lower end. They are also connected to the messenger wire just above the signal units. In light winds the weight of the signals is taken by the catenary wire and swinging of the signals is restrained by the messenger wire. In strong winds the combination of drag and lift forces on the signal units can result in substantial movement of the signals and changes in wire tension. To study the response of these types of system in strong winds the Florida State Department of Transportation has sponsored a research program at the Wall of Wind laboratory at Florida International University. The paper describes the development of a test rig that allows the non-linear response of the full scale signals to real wind conditions to be studied as a function of wind speed and direction. Preliminary results are also described, including the identification of an aerodynamic instability that can cause large amplitude oscillations of the whole signal system. The onset speed for the instability is a function of a number of parameters but most important are the signal geometry, the hanger design and the wire span.

Keywords: traffic signals, wind loading, wind tunnel testing, testing methods

1. INTRODUCTION

Traffic signals are an important part of the infrastructure and damage to them in wind storms disrupts the flow of traffic and creates unsafe conditions until they are repaired. The costs and delays for repair can be very significant (Sivarao et al., 2010). While many traffic signals are mounted on mast arms or overhead bridge structures, there are a significant number that are mounted on span wire systems, which are more economical. In the past a number of studies have been carried out on traffic signal structures supported on cantilevered masts (Kaczinski et al., 1996). For instance, McDonald et al., 1995 found that structural damage was caused by excessive wind-induced oscillations. Hamilton et al., 2000 developed a damping device to reduce vibration on traffic signals hanging from cantilever masts. However, most previous studies were restricted to traffic signals supported by cantilevered masts

at wind speeds below 100 mph (44.7 m/s). Existing standards such as ASCE 7-10 and AASHTO 2013 do not provide guidelines for wind loads on span-wire traffic signals. In 2003-2004, hurricanes with wind speeds exceeding 100 mph caused considerable damage to traffic signals in Florida, USA (Cook et al., 2012).

Therefore research has been initiated at Florida International University (FIU), funded by the Florida Department of Transportation (FDOT) to develop a better understanding of the mechanisms of failure of span wire signals and to develop more wind resistant systems. To do this a test rig has been developed at the Wall of Wind facility at FIU for studying the response to wind of span wire mounted signals. The overall program includes full scale tests and aero-elastic model simulations at 1:10 scale. This paper focuses on the design of the test rig and provides examples of early results obtain with it.

2. THEORETICAL BACKGROUND

The research so far conducted at FIU has focused on a span-wire arrangement shown schematically in Figure 1. In Figure 1only a single signal is shown to illustrate the general configuration, but typically the configurations studied had several signals fairly closely spaced. In zero wind the weight of the signals is taken by the Catenary Wire and the Messenger Wire is horizontal with some pretension applied. The tensions in the Catenary Wire are dictated by the weight of the signals, the sag ratio δ / L and the location of the signal along the wire. Here $\delta =$ sag and $L =$ total span.

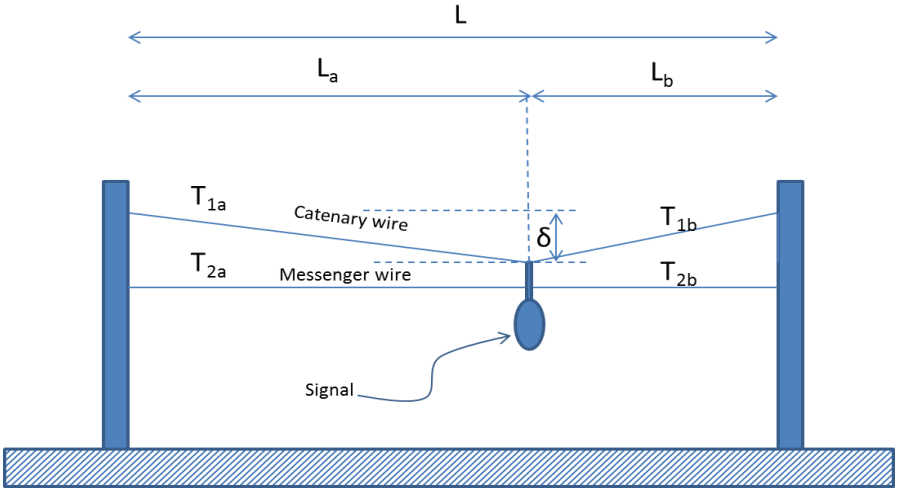

Figure 1: Schematic illustration of span-wire traffic signal system

Consider a wire tensioned between two anchor points as shown in Figure 2. This can be thought of as the messenger wire. If a force F_n is applied normal to its span (either vertically or horizontally) at the point of attachment of the signal/hanger system, for small deflections the difference in tensions T_a and T_b in the two parts of the span is negligible and they can be replaced by a single tension T . Then the balance of forces can be shown to be given to close approximation by

$$[1] \qquad F_n = T\left(\frac{L}{L_a L_b}\right)x_n$$

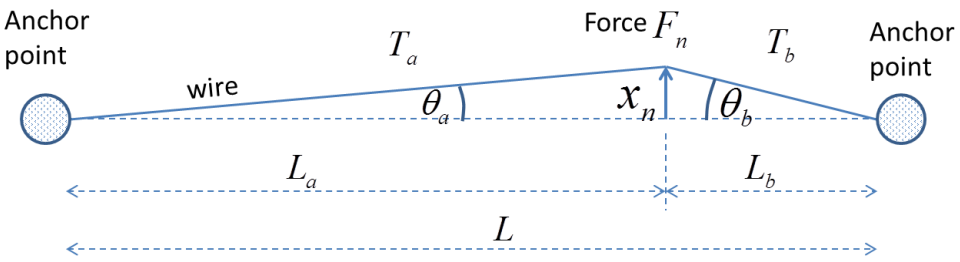

Figure 2: Deflection of wire due to application of force normal to span

For small deflections (e.g. $\frac{x_n}{L_a} < 0.1$) the following expression for the strain in the wire can also be derived

[2] $$\varepsilon = \frac{1}{2}\left[\frac{L^2}{L_a L_b}\right]\left(\frac{x_n}{L}\right)^2$$

The change in the wire tension ΔT is related to the strain by

[3] $$\Delta T = EA\varepsilon$$

where $E =$ modulus of elasticity of the wire and $A =$ effective cross-sectional area of the wire. From this it follows that the total tension is

[4] $$T = T_0 + \Delta T = T_0 + EA\frac{1}{2}\left[\frac{L^2}{L_a L_b}\right]\left(\frac{x_n}{L}\right)^2$$

where $T_0 =$ initial wire tension before application of the normal force F_n. Combining this with Equation 1 we deduce that the relationship between normal force F_n and deflection x_n is

[5] $$F_n = 4\frac{T_0}{L}Px_n + 8\frac{EA}{L^3}P^2x_n^3$$

In this relationship we introduced the position factor P defined as

[6] $$P \equiv \frac{L^2}{4L_a L_b}$$

For the case where the force is applied at mid-span $P = 1$ and the force-deflection relationship becomes

[7] $$F_n = 4\frac{T_0}{L}x_n + 8\frac{EA}{L^3}x_n^3$$

These relationships show that the force-deflection relationship is non-linear. As an example, suppose we have 3/8" diameter wire, for which the value of $EA = 0.81\times10^6$ lb. (3.61×10^6 N) is estimated, and that the span is $L = 84$ ft. (25.6 m). For 3/8" (9.5 mm) diameter wire the FDOT specified pretension is $T_0 = 286$ lb. (1273 N). Therefore for this case Equation 7 tells us that at mid span

[8] $$F_n = 13.6\,x_n + 10.9\,x_n^3 \text{ lb.}$$

where x_n is in feet. So for 1 ft. (0.305 m) deflection the force is 24.5 lb. (109 N) nearly half of which comes from the second non-linear term.

3. TEST RIG USING SPRINGS

In designing a test rig for full scale testing it is desirable to use a shorter span than in the field because this facilitates rotating the entire rig within the wind field of the test facility so as to explore the effect of various wind directions relative to the span. However, it is important in doing this that the span-wire possesses the same deflection versus force relationship as the field span. This can be achieved as follows. In the field the signals can be at various positions along the span but in the rig at the Wall of Wind test facility it is more practical to set up the signals so that they are symmetrically disposed about mid-span.

In Equation 5 we see that the coefficient of x_n in the first term on the right hand side is $4\frac{T_0}{L}P$. We want this coefficient to be the same on the rig as in the field. This will be achieved if we set the initial tension $T_{0,R}$ in the rig such that

[9] $$T_{0,R} = \frac{P_R L_R}{P_F L_F} T_{0,F}$$

where subscripts *R* and *F* denote the rig and field quantities respectively.

The coefficient of the second term in Equation 5 is $8\frac{EA}{L^3}P^2$ and, in order to achieve the same force versus deflection relationship as in the field, we need to devise a way of achieving an "effective" EA value, AE_{eff}, in the rig so that

[10] $$EA_{eff} = \left(\frac{L_{RIG}}{L_{FIELD}}\right)^3 \frac{P_F^2}{P_R^2} EA_F$$

As indicated earlier, in the rig we would generally have the signal unit at the center of the span or, if there are more than one signal units, they would be arranged in symmetrically about the center. So we consider the force-deflection relationship on the rig at the center of the span, implying $P_R = 1$. If we insert springs near each end of the wire in the rig as shown in Figure 3, the extension of the wire plus springs when the tension is increased by ΔT is

[11] $$\delta L = \frac{L_{wire}\Delta T}{EA_{RIG}} + 2\frac{\Delta T}{k}$$

where L_{wire} is the length of the wire in the rig after subtracting the length occupied by the springs. We want δL to be the same as would occur without springs but with a rig wire and spring combination that has an effective EA value given by Equation 10. Therefore from Equations 10 and 11

[12] $$\frac{L_{wire}\Delta T}{EA_R} + 2\frac{\Delta T}{k} = \frac{L_R \Delta T}{EA_{eff}} = \frac{L_R \Delta T}{\left(\frac{L_R}{L_F}\right)^3 P_F^2 EA_F}$$

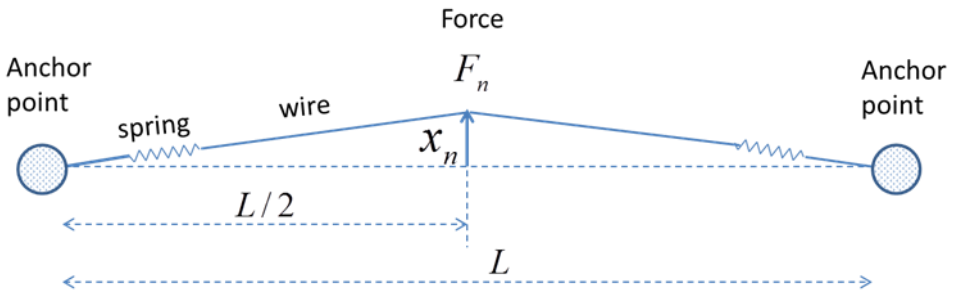

Figure 3: Use of springs to represent longer span

From this equation it can be deduced that the required spring stiffness is

$$[13] \qquad k = \frac{2\left(\frac{L_R}{L_F}\right)^3 P_F^2 \frac{EA_F}{L_R}}{1-\left(\frac{L_R}{L_F}\right)^3 P_F^2 \frac{EA_F L_{WIRE}}{EA_R L_R}}$$

In the rig set up the same diameter wire can be used as in the field, so that $EA_F / EA_R = 1$. Also, the factor $\left(L_{RIG} / L_{FIELD}\right)^3$ in the WOW test rig is typically 1/64 (the rig span is nominally 21 ft. (6.40 m) or smaller and L_{WIRE} / L_R is less than 1.0. Also, provided the signals in the field are not very close to the end of the span P_F is in the range of 1 to 2. These facts combine to make the denominator in Equation 23 very close to 1.0. Therefore for practical purposes the following simpler relationship can often be used to acceptable engineering accuracy

$$[14] \qquad k \approx 2\left(\frac{L_R}{L_F}\right)^3 P_F^2 \frac{EA_F}{L_R}$$

From this expression we see that if the signals in the field are offset from the center of the span then the required spring stiffness will go up according the square of the position factor, i.e. P_F^2. The minimum value of P is 1.0 which occurs when the signal position is at mid-span. However, if the signal is at the 1/3rd span position, for example, which might be more typical, then P_F^2 =1.27.

The messenger wire has the same force-deflection relationships for horizontal and vertical deflections. Therefore, provided the initial messenger wire tension is set according to Equation 9 and that the spring stiffness is set according to Equations 13 or 14, the non-linear stiffness at the point of attachment of the signal unit to the messenger wire will be correctly simulated for both horizontal and vertical deflections.

4. TREATMENT OF CATENARY WIRE

The case of the catenary wire is depicted in Figure 4. The initial tension T_0 is in this case the result of the built in sag δ and the weight Mg, where M = mass of signal and g = gravitational acceleration. The balance of vertical forces for small sag ratio δ / L may be written

$$[15] \qquad Mg = T_0\left(\frac{L^2}{L_a L_b}\right)\frac{\delta}{L} = 4T_0 P \frac{\delta}{L}$$

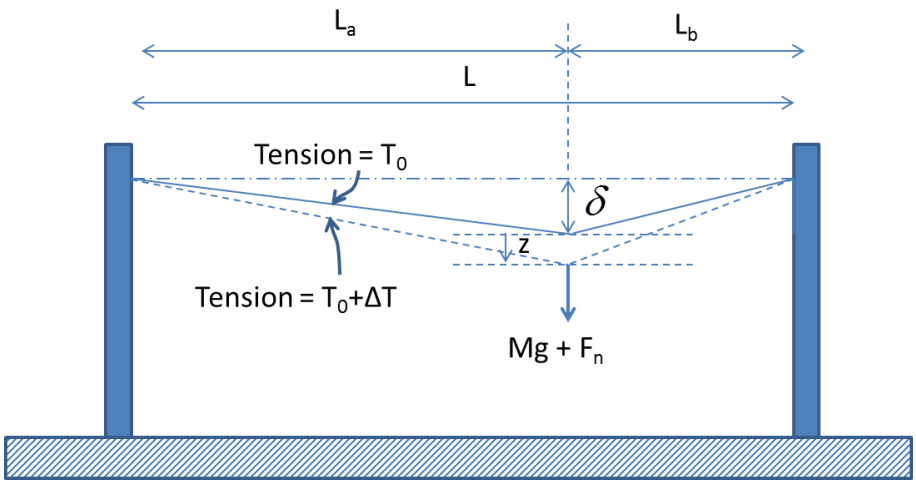

Figure 4: Catenary deflections

When the additional vertical force F_n is applied the balance of forces for small sags becomes

[16] $$Mg + F_n = (T_0 + \Delta T).4P\frac{\delta + z}{L}$$

Using Equation 15 and following a similar analysis as used for the messenger wire, the following force-deflection relationship for vertical deflections can be obtained.

[17] $$F_n = \frac{Mg}{\delta}z + \frac{8EA}{L^3}P^2(z^3 + 3z^2\delta + 2z\delta^2)$$

Therefore on the rig we can obtain the same relationship between vertical force and deflection as in the field provided we satisfy two criteria which are:

1. The sag distance δ is kept the same as in the field. This ensures that the coefficient of z in the first term in Equation 17 is kept the same as in the field. It also ensures that the coefficients of z^2 and z in the brackets of the second term in Equation 17 are kept the same as in the field.
2. The parameter $\frac{EA}{L^3}P^2$ is kept the same as in the field, which can be achieved in the same way as for the messenger wire, by using springs to obtain an effective value of EA which is scaled down in proportion to L^3 / P^2.

The spring stiffness requirement is the same as for the messenger wire and the sag requirement is met by simply maintaining the same sag distance δ, rather than sag ratio δ / L, as in the field. For small deflections the horizontal force-deflection relationship for the catenary wire is the same as for the messenger wire resulting in the same spring stiffness again. The above results for the force-deflection relationships are consistent with those of Irvine, 1974 and Inglis, 1963.

5. IMPLEMENTATION

Based on the above analysis a test rig has been constructed consisting of two posts supported on a common stiff base structure, with the span wires connected to the two posts. Coil springs are inserted into the span wires near the posts. Figure 5 illustrates the set up in the Wall of Wind (WOW) facility, a description of which can be found in

Mooneghi et al., 2014. The test rig span is 21 ft. (6.40 m) which allows the entire rig to be rotated on the test facility's turntable so as to examine the effects of different wind directions. Six component load cells measure the forces at the connections of the span wires to the end posts. Additional instrumentation in the form of accelerometers, tilt meters and orientation sensors is installed in the signal units to provide further information on signal angular deflections and accelerations as a function of wind speed and direction. High definition video recordings of the tests are also obtained.

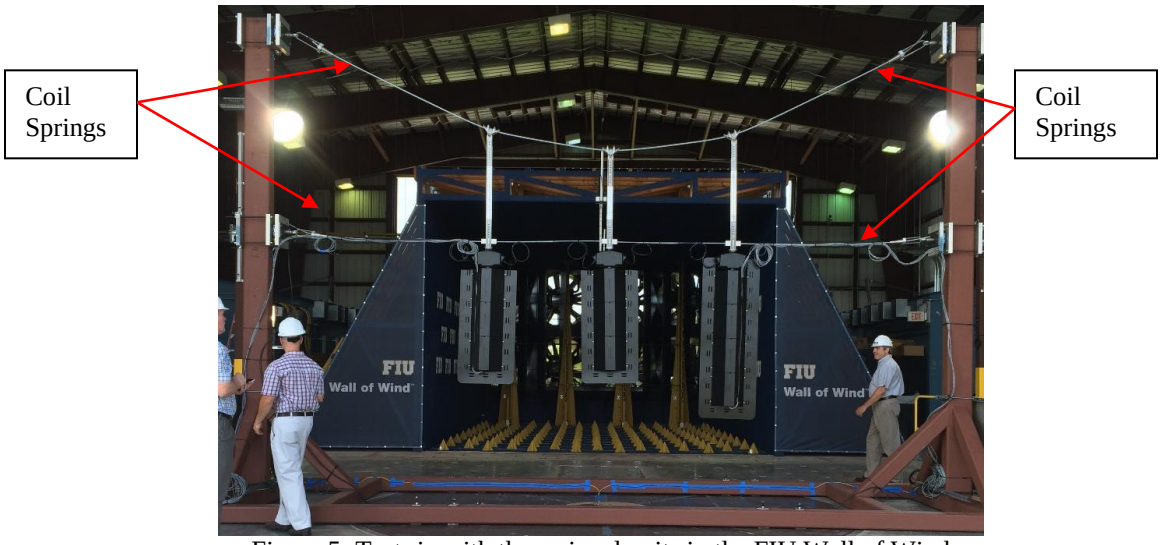

Figure 5: Test rig with three signal units in the FIU Wall of Wind

Since the tests are at full scale it is not possible to simulate the complete turbulence spectrum of the wind. Therefore there is a choice of either testing in non-turbulent flow or in a flow with high frequency turbulence that is representative of high frequency turbulence in the natural wind. The latter approach has been taken to date using turbulence with integral scale of 1.5 ft. and intensity of 7%. The high frequency turbulence has been estimated to be representative of that found in suburban terrain. Some initial tests have been undertaken on various types of hanger and signal systems. Some hanger designs have a rigid rod connected to the catenary and messenger wires and continuing down to a rigid connection to the signal unit. Others have various types of flexible joint just above the messenger wire.

6. PRELIMINARY RESULTS AND DISCUSSION

Figure 6 shows examples of two types of hanger for which some illustrative results are described here. The first, denoted as Case 1 has a flexible joint just above the messenger wire. The second has a continuous nominally rigid strap running from Catenary down to the signal unit. The wind direction for the results discussed below was normal to the span and impacted the front face of the signals. The springs used in these tests had a spring constant of 100 lb./in (175 N/cm) which made the rig span of 21 ft (6.4 m) behave like a field span of 84 ft. (25.6 m). Figure 7 shows the location of the load cells, inclinometers and accelerometers used to measure the forces, inclinations and accelerations respectively.

a) b)

Figure 6: Cases tested in the WOW at FIU: a) Case 1 – flexible joint in strap; b) Case 2 – nominally rigid strap

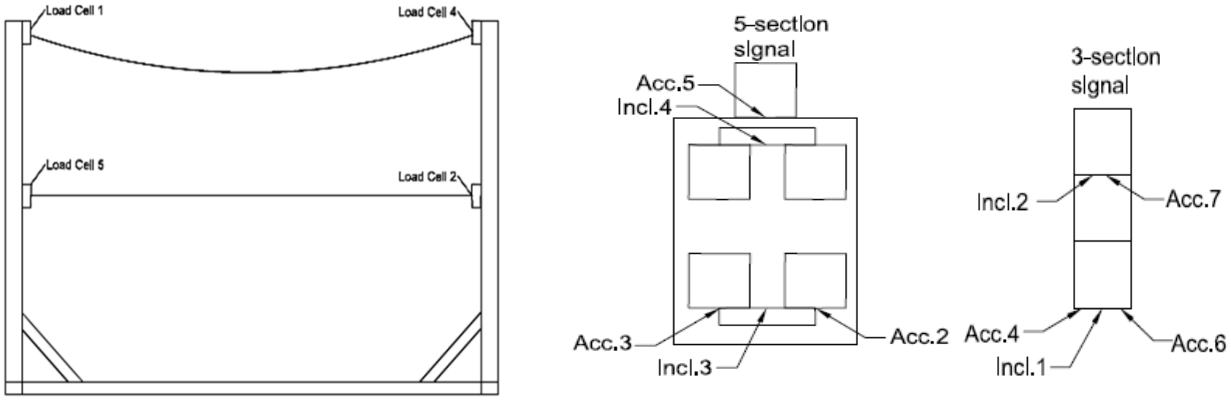

Figure 7: Location of load cells, accelerometers and inclinometers (after Zisis et al., 2016)

Figures 8 shows measurements of the span-wire tensions (30 second averages) as a function of wind speed for Case 1. It can be seen that the Catenary tensions are generally much lower than in the Messenger wire. The tensions do not go up in proportion to speed squared because the signals blow back thus reducing frontal area. Large amplitude oscillations persisted over a range of speeds for Case 1 as can be seen in Figure 9 which shows acceleration measurements.

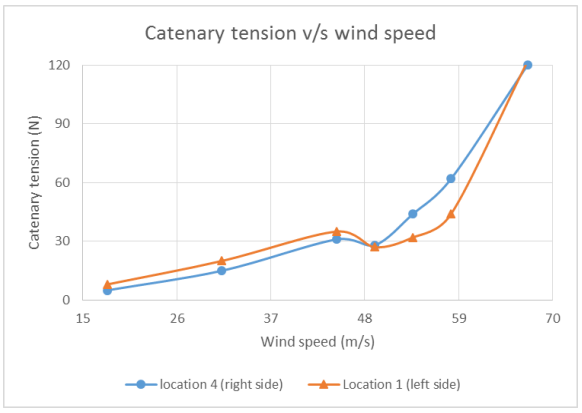

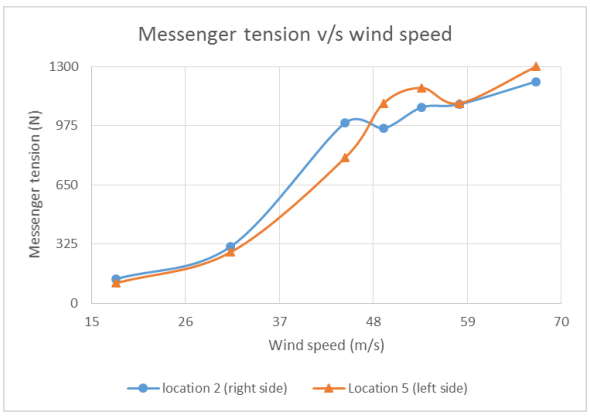

a) b)

Figure 8: Case 1 span-wire tensions as function of wind speed: a) Catenary wire; b) Messenger wire

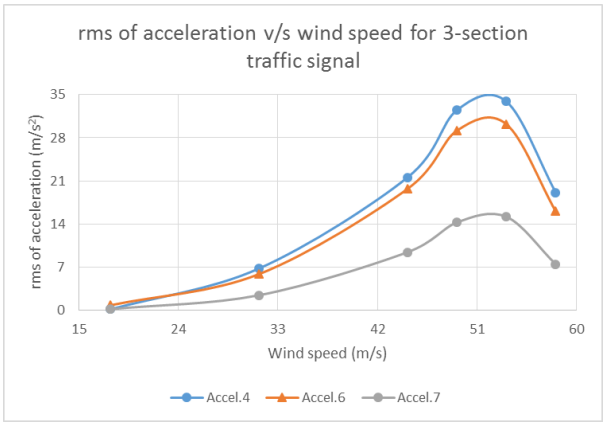

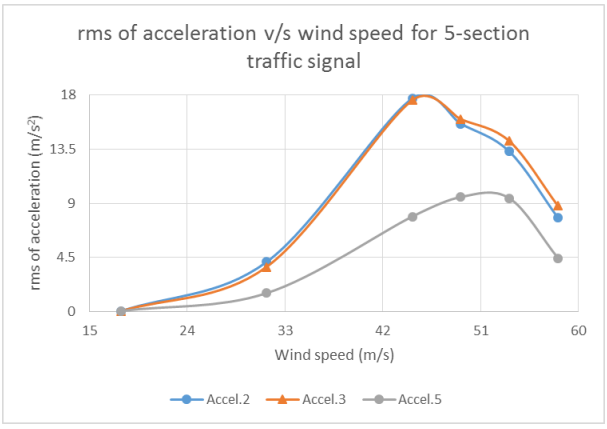

a) b)

Figure 9: Rms accelerations as function of wind speed for Case 1: a) 3-section traffic signal; b) 5-section traffic signal

It can be seen in Figure 9 that rms accelerations reached values as high as 35 m/s^2 on the three section signal and 18 m/s^2 on the 5 section signal for the Case 1 hangers. The oscillations signified by these high accelerations began at about 31 m/s and persisted over a range of speeds up to 58 m/s beyond which the accelerometers were removed to preserve them in the event that the signals broke from the wires at higher speeds. It should be noted that the thin aluminum back plates on the signals typically were partially or wholly torn off well before the maximum test speed was reached and the aerodynamics of the signals would have been changed as a result.

Figures 10 and 11 show results for Case 2. The wire tensions were similar in magnitude to Case 1 but the accelerations were an order of magnitude less and remained below 3 m/s^2. The acceleration measurements were consistent with visual observations and video recordings that oscillations were substantially less than for Case 1.

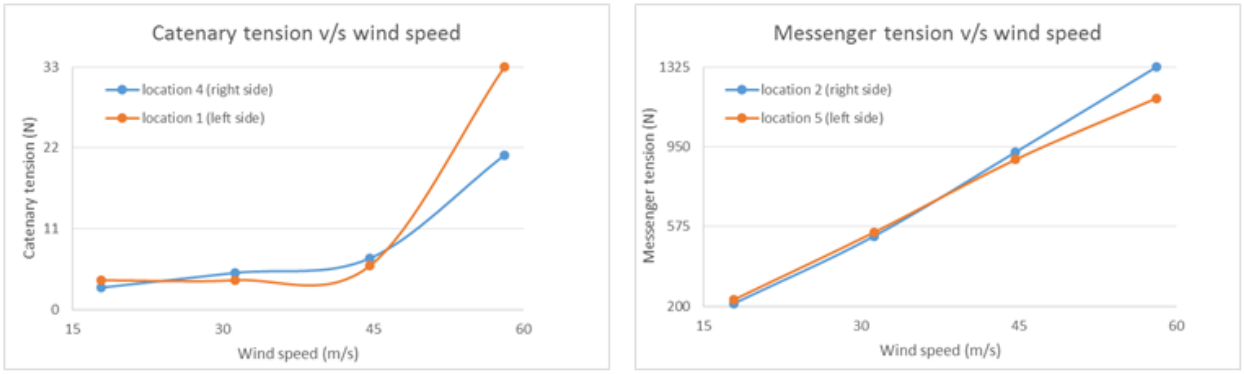

a) b)

Figure 10: Tensions in the cables for Case 2: a) Catenary wire; b) Messenger wire

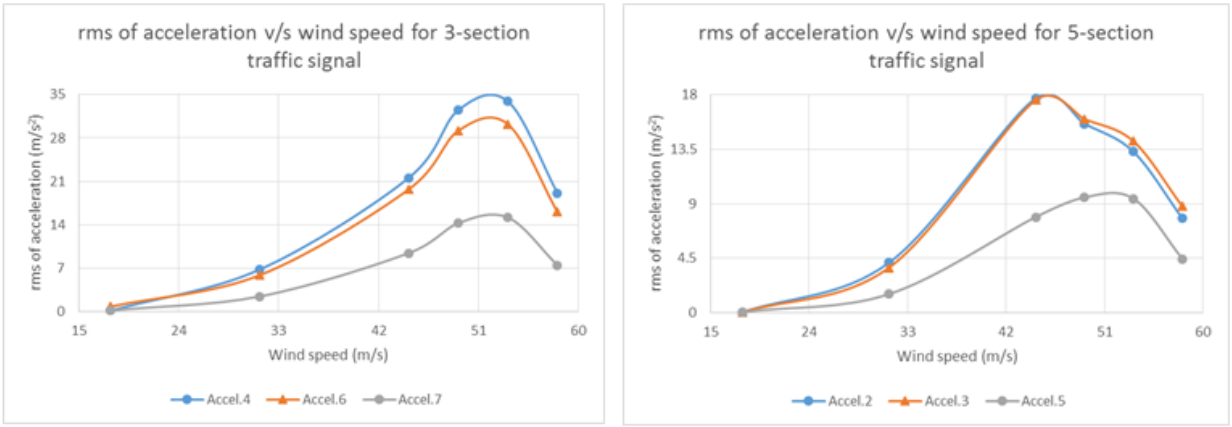

a) b)

Figure 11. Rms accelerations as function of wind speed for Case 2: a) 3-section traffic signal; b) 5-section traffic signal

7. CONCLUSIONS

The analysis of the non-linear force versus deflection relationships for tensioned span wires indicate that on a test rig of much shorter span than the real span in the field it is possible to still obtain the same non-linear stiffness behaviour as in the field. This can be achieved by introducing springs into span wires on the rig. Expressions for the required spring constant are derived. In addition to the using the springs the pretension in the Messenger wire needs to be reduced in proportion the span and on the Catenary wire the sag distance δ needs to be maintained the same as in the field (rather than the sag ratio δ / L). Preliminary tests have been undertaken on a number of signal configurations. The examples of results in the paper show that the design of the hanger can have important effects on the dynamic response of the signals. Signals that had hangers with a flexible link between the Messenger and the Catneary wires tended to go into large amplitude oscillations over a range of speeds whereas signals without a flexible link exhibited much smaller oscillations.

8. ACKOWLEDGEMENTS

The test rig described in this paper is part of a research program funded by Florida Department of Transportation (FDOT). The support and encouragement from the Traffic Engineering Research Lab of FDOT is gratefully acknowledged. The opinions, findings and conclusions expressed in this publication are those of the authors and not necessarily those of the Florida Department of Transportation or the U.S. Department of Transportation. Also, the staff of the Wall of Wind, Walter Concklin and Roy Lui-Marques, played key roles in the rig set up, the

instrumentation and running of the tests. Their importatnt contributions are acknowledged. Finally, the authors would like to thank Horsepower Electric Inc. electrical contractors for their unstinting support in providing experienced teams for the installation of traffic signals and changing equipment between tests.

REFERENCES

ASCE 7-10, Minimum Design Loads for Buildings and Other Structures, *American Society of Civil Engineers, ASCE*, 2010, Virginia, USA.

AASHTO, American Association of state Highway and Transportation Officials, Standard specifications for structural supports for highway signs, luminaires and traffic signals, 6th edition, Washington, USA, 2013.

Cook, R.A., Masters, F., Rigdon, J.L. 2012. Evaluation of Dual Cable Signal Support Systems with Pivotal Hanger Assemblies. *FDOT Contract No. BDK75 977-37, University of Florida, Department of Civil and Coastal Engineering*, 2012, Gainesville, FL, USA.

Hamilton, HR, Riggs GS, Puckett JA. Increased damping in cantilevered traffic signal structures. *Journal of Structural Engineering*. 2000, Apr, 126 (4):530-7.

Irvine, H.M., Studies in the Statics and Dynamics of Simple Cable Systems, California Institute of Technology, Dynamics Laboratory Report, 1974, DYNL-108.

Inglis, C., Applied Mechanics for Engineers, Dover Publications, 1963, New York, USA.

Kaczinski MR, Dexter RJ, Van Dien JP. Fatigue-resistant design of cantilevered signal, sign and light supports. *Transportation Research Board, NCHRP report 412, National Research Council*; 1998.

McDonald J.R., Mehta, K. C., W. Oler, and N. Pulipaka. Wind load effects on signs, luminaires and traffic signal structures. *Report 1303-1F, Department of Transportation, Texas*, 1995, USA.

Mooneghi, M. A., Irwin, P., Chowdhury, A. G. Large-scale testing on wind uplift of roof pavers, *Journal of wind engineering and industrial aerodynamics*, 128, 2014, 22-36.

Sivarao SK, Esro M, Anand TJ. Electrical & Mechanical Fault Alert Traffic Light System Using Wireless Technology. *International Journal of Mechanical and Mechatronics Engineering*. 2010; 10(4):19-22.

Zisis, I., Irwin, P., Chowdhury, A., Azizinamini, A., Berlanga, B. Development of a Test Method for Assessing the Performance of Vehicular Traffic Signal Assemblies during Hurricane Force Winds, *Report no. BDV29 TWO 977-20*, 2016, FDOT, Fl, USA.